Phase diagrams in mixed spin-3/2 and spin-2 Ising system with two alternative layers within the effective-field theory*

Bayram Deviren[a)], Yasin Polat[b)], and Mustafa Keskin[c)†]

[a)] *Department of Physics, Nevsehir University,* 50300 *Nevşehir, Turkey*
[b)] *Institute of Science, Erciyes University,* 38039 *Kayseri, Turkey*
[c)] *Department of Physics, Erciyes University,* 38039 *Kayseri, Turkey*

(Received 12 November 2010; revised manuscript received 17 January 2011)

The phase diagrams in the mixed spin-3/2 and spin-2 Ising system with two alternative layers on a honeycomb lattice are investigated and discussed by the use of the effective-field theory with correlations. The interaction of the nearest-neighbour spins of each layer is taken to be positive (ferromagnetic interaction) and the interaction of the adjacent spins of the nearest-neighbour layers is considered to be either positive or negative (ferromagnetic or antiferromagnetic interaction). The temperature dependence of the layer magnetizations of the system is examined to characterize the nature (continuous or discontinuous) of the phase transitions and obtain the phase transition temperatures. The system exhibits both second- and first-order phase transitions besides triple point (TP), critical end point (E), multicritical point (A), isolated critical point (C) and reentrant behaviour depending on the interaction parameters. We have also studied the temperature dependence of the total magnetization to find the compensation points, as well as to determine the type of behaviour, and N-type behaviour in Néel classification nomenclature existing in the system. The phase diagrams are constructed in eight different planes and it is found that the system also presents the compensation phenomena depending on the sign of the bilinear exchange interactions.

Keywords: mixed spin-3/2 and spin-2 Ising system, effective-field theory, compensation phenomena, phase diagrams

PACS: 05.50.+q, 05.70.Fh, 64.60.De, 75.10.Hk **DOI:** 10.1088/1674-1056/20/6/060507

1. Introduction

Over the last few decades, the magnetic properties of various magnetic multilayers, layered structure and thin films have attracted significant attention, because of their great potential for technological applications, such as the high-density magneto-optical recording. These materials also present interesting novel magnetic properties, such as giant magnetoresistance, surface magnetic elastic coupling, enhanced surface magnetic moment and surface magnetic anisotropy. Experimentally, the structural and magnetic properties of the multilayers were investigated, such as Fe/Ni,[1] Fe/Ni and Fe/Co,[2] Ni/Au,[3] Co/Cu/$Ni_{80}Fe_{20}$.[4] Theoretically, progressive attention has been paid to the examination of the spin arrangement as well as the types of couplings governing the magnetic behaviour of these systems. In order to obtain a theoretical understanding of various phenomena that arise from these materials, it is instructive to consider simple models such as the two-sublattice Ising model that allows us to calculate exactly or realistically observable quantities.[5] Most of these studies related to magnetic multilayer systems have been restricted to Ising or Heisenberg systems consisting of only spin-1/2 where each layer has a coupling constant of a different magnitude.[6−8] The restriction on only spin-1/2 is too idealized. It is necessary to discuss magnetic multilayers with higher and different spins.

On the other hand, higher and mixed spin systems, also called the extended Ising systems, are still an interesting subject of study because new behaviours, such as the tricritical points and the reentrant phenomenon, have been observed, which are not the case where pure spin-1/2 or the conventional Ising model holds. In particular, because of the syntheses of many new magnets like the poly-layer magnet, the thin-film magnet and the molecular-based magnet, the

*Project supported by the Scientific and Technological Research Council of Turkey (TÜBİTAK) (Grant No. 107T533) and Erciyes University Research Funds (Grant No. FBD-08-593).

†Corresponding author. E-mail: keskin@erciyes.edu.tr

© 2011 Chinese Physical Society and IOP Publishing Ltd

emphasis has been placed on the layered mixed spin Ising model.[9] Most of these studies were confined to layered mixed spin-1/2 and spin-S Ising system because of its relative simplicity and its similarity to many layered magnets (see Refs. [10]–[12] and the references therein). There are also a few investigations on the layered mixed spin Ising system consisting of both high spins.[13,14] However, many more complicated magnets with many high spins have been synthesized recently; therefore the theoretical studies with many high spins should be extended. Moreover, one of the high mixed spin Ising systems is the spin-3/2 and spin-2 mixed system besides the mixed spins Ising systems with spins (1, 1/2) with spins (1/2, 3/2), with spins (1, 3/2). An early attempt to study the mixed spin-3/2 and spin-2 Ising model with a crystal-field interaction was made by Bobák and Dely[15] within the framework of a mean-field theory (MFT) based on Bogoliubov inequality for the free energy. They presented the phase diagrams and found that the system exhibits the tricritical point, triple point and isolated critical point. Albayrak[16] also studied the mixed spin-3/2 and spin-2 Ising system with two different crystal-field interactions on the Bethe lattice by using the exact recursion equations. He calculated the phase diagrams and found that the system only contains the tricritical point and isolated critical point. Recently, phase transitions and multicritical points in the mixed spin-3/2 and spin-2 Ising model with different single-ion anisotropies were studied by the use of a mean-field theory based on the Bogoliubov inequality for the Gibbs free energy by Miao *et al.*[17]

Despite these studies, as far as we know, the mixed spin-3/2 and spin-2 Ising system with alternative layers on honeycomb lattice has not been investigated. Therefore, the purpose of the present work is to study the magnetic behaviour of the mixed spin-3/2 and spin-2 Ising system with alternative layers on honeycomb lattice with crystal-field interaction by the use of the effective-field theory (EFT) with correlations. The temperature dependence of the layer magnetizations of the system is examined to characterize the nature (continuity or discontinuity) of the phase transitions and obtain the phase transition temperature. The temperature dependence of the total magnetization is also investigated to find the compensation points, as well as to determine the type of behaviour. The phase diagrams are constructed in seven different planes and we find that the system exhibits both second- and first-order phase transitions besides triple point (TP), critical end point (E), multicritical point (A) and isolated critical point (C), which depend on the interaction parameters. It is worth while mentioning that the EFT can include some effects of spin–spin correlations by using the van der Waerden identity and it provides the results that are much superior to those obtained within the MFT.[18] The EFT has been successfully applied to a variety of Ising spin problems and a good review has been found in Ref. [19]. Finally, we should also mention that this mixed spin (3/2, 2) system corresponds to the Prussian blue of the type $Fe^{II}_{1.5}[Cr^{III}(CN)_6]\cdot nH_2O$.[20]

The outline of the rest of the paper is as follows. In Section 2, we introduce briefly the basic framework of the EFT with correlations and give the formulation for the mixed spin-3/2 and spin-2 Ising system with alternative layers on the honeycomb lattice. The detailed numerical results and discussion are given in Section 3, followed by a brief summary.

2. Formulation

We consider a mixed spin-3/2 and spin-2 Ising system with alternative layers on a honeycomb lattice. The lattice is formed by alternate layers of σ and S spins; hence the two different types of spins are described by Ising variables, which can take the values $\sigma = \pm 3/2,\ \pm 1/2$ and $S = \pm 2,\ \pm 1,\ 0$. The σ and S spins are distributed in alternate layers of a honeycomb lattice as seen in Fig. 1 where A and B layers are occupied by spins σ and S, respectively. In Fig. 1, open and solid circles represent σ and S spins, respectively. The Hamiltonian of the system is given by

$$\begin{aligned}\mathscr{H} = & -J_{\rm a}\sum_{\langle ij\rangle}\sigma_i\sigma_j - J_{\rm b}\sum_{\langle mn\rangle}S_mS_n - J_{\rm ab}\sum_{\langle im\rangle}\sigma_i{\rm S}_m \\ & -\Delta\left(\sum_i\sigma_i^2+\sum_m S_m^2\right) \\ & -h\left(\sum_i\sigma_i+\sum_m S_m\right), \end{aligned} \tag{1}$$

where the first three summations are carried out only over nearest-neighbour pairs of spins, i.e., $\langle ij\rangle$, $\langle mn\rangle$, and $\langle im\rangle$. J_a and $J_{\rm b}$ are the intralayer coupling constants taken to be positive, i.e., couplings between the spins, σ–σ and S–S, in each of the layer are assumed to be ferromagnetic. $J_{\rm ab}$ is the interlayer coupling constant of the adjacent σ–S spins of the layers between A and B, which is taken to be either positive or negative;

thus, ferromagnetic or anti-ferromagnetic coupling between the layers is assumed. Δ is the crystal–field interaction or a single-ion anisotropy constant and h represents the longitudinal magnetic field.

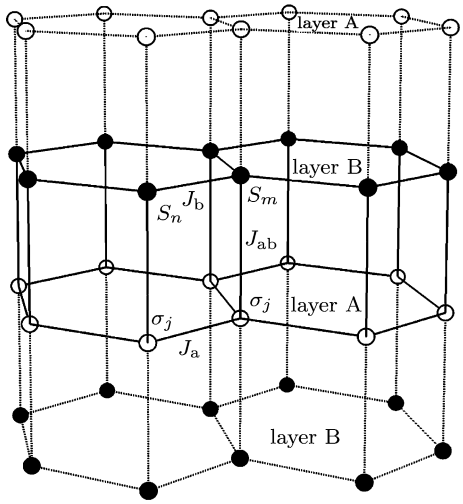


Fig. 1. Sketch of the alternative layers. J_a and J_b each are the intralayer coupling constant of each layer and J_{ab} is the interlayer coupling constant of the adjacent spins of the layer between A and B. The open (◯) and solid circle (•) denote the spins of $\sigma_i = 3/2$ and $S_m = 2$, respectively, for honeycomb lattice.

The problem is now to evaluate the mean values $m_A = \langle \sigma_i \rangle$ and $m_B = \langle S_m \rangle$. The starting point for statistics of the present spin system is the exact relation.[21] As discussed in Ref. [22], for the evaluation of mean values $\langle \sigma_i \rangle$ and $\langle S_m \rangle$ we can use the exact Ising spin identities and the differential operator technique introduced by Honmura and Kaneyoshi.[23] Within the framework of the EFT, the magnetizations per A and B layers are given by

$$\begin{aligned}\langle \sigma_i^k \rangle = & \Bigg\langle \prod_{i=1}^{z_1} \{A(J_a \nabla) + B(J_a \nabla)\, \sigma_i \\ & + C(J_a \nabla)\, \sigma_i^2 + D(J_a \nabla)\, \sigma_i^3\} \\ & \times \prod_{m=1}^{z_2} \{1 + K(J_{ab} \nabla)\, S_m L(J_{ab} \nabla)\, S_m^2 \\ & + M(J_{ab} \nabla)\, S_m^3 + N(J_{ab} \nabla)\, S_m^4\} \Bigg\rangle f_k(x)\,|_{x=0}, \end{aligned} \tag{2}$$

$$\begin{aligned}\langle S_m^k \rangle = & \Bigg\langle \prod_{m=1}^{z_1} \{1 + K(J_b \nabla)\, S_m L(J_b \nabla)\, S_m^2 \\ & + M(J_b \nabla)\, S_m^3 + N(J_b \nabla)\, S_m^4\} \\ & \times \prod_{i=1}^{z_2} \{A(J_{ab} \nabla) + B(J_{ab} \nabla)\, \sigma_i \\ & + C(J_{ab} \nabla)\, \sigma_i^2 + D(J_{ab} \nabla)\, \sigma_i^3\} \Bigg\rangle g_k(x)\,|_{x=0}, \end{aligned} \tag{3}$$

where $\nabla = \partial/\partial x$ is the differential operator. If one defines z_1 as the coordination number that nearest-neighbours of every spin on each layer and z_2 as the coordination number that the next nearest-neighbours of every spin are all the adjacent layers; hence $z_1 = 3$ and $z_2 = 2$ for the alternative layers on a honeycomb lattice, easily seen from Fig. 1. The functions $f_k(x)$ and $g_k(x)$ are defined by

$$f_1(x) = \frac{1}{2} \frac{3\,\sinh[3\,\beta(x+h)/2] + \sinh[\beta(x+h)/2]\ \exp(-2\beta\,\Delta)}{\cosh[3\beta(x+h)/2] + \cosh[\beta(x+h)/2]\ \exp(-2\beta\,\Delta)}, \tag{4a}$$

$$f_2(x) = \frac{1}{2} \frac{9\,\cosh[3\,\beta(x+h)/2] + \cosh[\beta(x+h)/2]\ \exp(-2\beta\,\Delta)}{2\cosh[3\beta(x+h)/2] + 2\cosh[\beta(x+h)/2]\ \exp(-2\beta\,\Delta)}, \tag{4b}$$

$$f_3(x) = \frac{1}{2} \frac{27\,\sinh[3\,\beta(x+h)/2] + \sinh[\beta(x+h)/2]\ \exp(-2\beta\,\Delta)}{4\cosh[3\beta(x+h)/2] + 4\cosh[\beta(x+h)/2]\ \exp(-2\beta\,\Delta)}; \tag{4c}$$

$$g_1(x) = \frac{1}{2} \frac{4\,\sinh[2\beta(x+h)] + 2\,\sinh[\beta(x+h)]\ \exp(-3\beta\,\Delta)}{\cosh[2\beta(x+h)] + \cosh[\beta(x+h)]\ \exp(-3\beta\,\Delta) + \exp(-4\beta\,\Delta)}, \tag{5a}$$

$$g_2(x) = \frac{1}{2} \frac{8\,\cosh[2\beta(x+h)] + 2\,\cosh[\beta(x+h)]\ \exp(-3\beta\,\Delta)}{\cosh[2\beta(x+h)] + \cosh[\beta(x+h)]\ \exp(-3\beta\,\Delta) + \exp(-4\beta\,\Delta)}, \tag{5b}$$

$$g_3(x) = \frac{1}{2} \frac{16\,\sinh[2\beta(x+h)] + 2\,\sinh[\beta(x+h)]\ \exp(-3\beta\,\Delta)}{\cosh[2\beta(x+h)] + \cosh[\beta(x+h)]\ \exp(-3\beta\,\Delta) + \exp(-4\beta\,\Delta)}, \tag{5c}$$

$$g_4(x) = \frac{1}{2} \frac{32\,\cosh[2\beta(x+h)] + 2\,\cosh[\beta(x+h)]\ \exp(-3\beta\,\Delta)}{\cosh[2\beta(x+h)] + \cosh[\beta(x+h)]\ \exp(-3\beta\,\Delta) + \exp(-4\beta\,\Delta)}, \tag{5d}$$

where $\beta = 1/kT$, k is the Boltzmann constant, T is the absolute temperature, the coefficients $A(J_a \nabla)$, $B(J_a \nabla)$, $C(J_a \nabla)$, $D(J_a \nabla)$, and $A(J_{ab} \nabla)$, $B(J_{ab} \nabla)$, $C(J_{ab} \nabla)$, $D(J_{ab} \nabla)$ for spin-3/2, and $K(J_b \nabla)$, $L(J_b \nabla)$, $M(J_b \nabla)$, $N(J_b \nabla)$, and $K(J_{ab} \nabla)$, $L(J_{ab} \nabla)$, $M(J_{ab} \nabla)$, $N(J_{ab} \nabla)$ for spin-2 are given in Appendix A.

The expressions (2) and (3) are also exact and are valid for any lattice. If we try to exactly treat all the spin–spin correlation for that set of equations, the problem quickly becomes intractable. A first obvious attempt to deal with it is to ignore correlations; the decoupling approximations:

$$\begin{aligned}\langle\sigma_i\ \sigma_i'^2\cdots\sigma_{i^n}^3\rangle &\cong \langle\sigma_i\rangle\langle\sigma_i'^2\rangle\cdots\langle\sigma_{i^n}^3\rangle\,,\\ \langle\,S_j\ S_j'^2\cdots S_{j^n}^4\rangle &\cong \langle S_j\rangle\langle S_j'^2\rangle\cdots\langle S_{j^n}^4\rangle\,,\end{aligned}\tag{6}$$

with $i\neq i'\neq\cdots\neq i^n$ and $j\neq j'\neq\cdots\neq j^n$ have been introduced within the effective-field theory with correlations.[23] In fact, the approximation corresponds essentially to the Zernike approximation[24] in the bulk problem and has been successfully applied to a great number of magnetic systems including the surface problems.[22,23] On the other hand, in the mean-field theory all the correlations, including the self-correlations, are neglected. Based on these approximations, equations (2) and (3) are reduced to

$$\begin{aligned}m_{\rm A} = [&(A(J_{\rm a}\nabla)+B(J_{\rm a}\nabla)\langle\sigma_i\rangle\\ &+C(J_{\rm a}\nabla)\langle\sigma_i^2\rangle+D(J_{\rm a}\nabla)\langle\sigma_i^3\rangle)^3\\ &\times(1+K(J_{\rm ab}\nabla)\langle S_m\rangle\\ &+L(J_{\rm ab}\nabla)\langle S_m^2\rangle+M(J_{\rm ab}\nabla)\langle S_m^3\rangle\\ &+N(J_{\rm ab}\nabla)\langle S_m^4\rangle)^2]f_1(x)\,|_{x=0},\end{aligned}\tag{7}$$

$$\begin{aligned}q_{\rm A} = [&(A(J_{\rm a}\nabla)+B(J_{\rm a}\nabla)\langle\sigma_i\rangle\\ &+C(J_{\rm a}\nabla)\langle\sigma_i^2\rangle+D(J_{\rm a}\nabla)\langle\sigma_i^3\rangle)^3\\ &\times(1+K(J_{\rm ab}\nabla)\langle S_m\rangle\\ &+L(J_{\rm ab}\nabla)\langle S_m^2\rangle+M(J_{\rm ab}\nabla)\langle S_m^3\rangle\\ &+N(J_{\rm ab}\nabla)\langle S_m^4\rangle)^2]f_2(x)\,|_{x=0},\end{aligned}\tag{8}$$

$$\begin{aligned}r_{\rm A} = [&(A(J_{\rm a}\nabla)+B(J_{\rm a}\nabla)\langle\sigma_i\rangle\\ &+C(J_{\rm a}\nabla)\langle\sigma_i^2\rangle+D(J_{\rm a}\nabla)\langle\sigma_i^3\rangle)^3\\ &\times(1+K(J_{\rm ab}\nabla)\langle S_m\rangle\\ &+L(J_{\rm ab}\nabla)\langle S_m^2\rangle+M(J_{\rm ab}\nabla)\langle S_m^3\rangle\\ &+N(J_{\rm ab}\nabla)\langle S_m^4\rangle)^2]f_3(x)\,|_{x=0},\end{aligned}\tag{9}$$

$$\begin{aligned}m_{\rm B} = [&(1+K(J_{\rm b}\nabla)\langle S_m\rangle+L(J_{\rm b}\nabla)\langle S_m^2\rangle\\ &+M(J_{\rm b}\nabla)\langle S_m^3\rangle+N(J_{\rm b}\nabla)\langle S_m^4\rangle)^3\\ &\times(A(J_{\rm ab}\nabla)+B(J_{\rm ab}\nabla)\langle\sigma_i\rangle\\ &+C(J_{\rm ab}\nabla)\langle\sigma_i^2\rangle+D(J_{\rm ab}\nabla)\langle\sigma_i^3\rangle)^2]\\ &\times g_1(x)\,|_{x=0},\end{aligned}\tag{10}$$

$$\begin{aligned}q_{\rm B} = [&(1+K(J_{\rm b}\nabla)\langle S_m\rangle+L(J_{\rm b}\nabla)\langle S_m^2\rangle\\ &+M(J_{\rm b}\nabla)\langle S_m^3\rangle+N(J_{\rm b}\nabla)\langle S_m^4\rangle)^3\\ &\times(A(J_{\rm ab}\nabla)+B(J_{\rm ab}\nabla)\langle\sigma_i\rangle\\ &+C(J_{\rm ab}\nabla)\langle\sigma_i^2\rangle+D(J_{\rm ab}\nabla)\langle\sigma_i^3\rangle)^2]\\ &\times g_2(x)\,|_{x=0},\end{aligned}\tag{11}$$

$$\begin{aligned}r_{\rm B} = [&(1+K(J_{\rm b}\nabla)\langle S_m\rangle+L(J_{\rm b}\nabla)\langle S_m^2\rangle\\ &+M(J_{\rm b}\nabla)\langle S_m^3\rangle+N(J_{\rm b}\nabla)\langle S_m^4\rangle)^3\\ &\times(A(J_{\rm ab}\nabla)+B(J_{\rm ab}\nabla)\langle\sigma_i\rangle\\ &+C(J_{\rm ab}\nabla)\langle\sigma_i^2\rangle+D(J_{\rm ab}\nabla)\langle\sigma_i^3\rangle)^2]\\ &\times g_3(x)\,|_{x=0},\end{aligned}\tag{12}$$

$$\begin{aligned}v_{\rm B} = [&(1+K(J_{\rm b}\nabla)\langle S_m\rangle+L(J_{\rm b}\nabla)\langle S_m^2\rangle\\ &+M(J_{\rm b}\nabla)\langle S_m^3\rangle+N(J_{\rm b}\nabla)\langle S_m^4\rangle)^3\\ &\times(A(J_{\rm ab}\nabla)+B(J_{\rm ab}\nabla)\langle\sigma_i\rangle\\ &+C(J_{\rm ab}\nabla)\langle\sigma_i^2\rangle+D(J_{\rm ab}\nabla)\langle\sigma_i^3\rangle)^2]\\ &\times g_4(x)\,|_{x=0}.\end{aligned}\tag{13}$$

So far we have discussed the basic formulation of the mixed spin-3/2 and spin-2 Ising system with a crystal–field in a longitudinal magnetic field; hence equations (7)–(13) can be used to investigate the thermal variations of the layer magnetizations and then phase diagrams can be calculated. As one can see, in our treatment new order parameters $q_{\rm A}$, $q_{\rm B}$, $r_{\rm A}$, $r_{\rm B}$, and $v_{\rm B}$ naturally appear which can be evaluated. This is not the case of the standard MFT where all correlations are neglected. This is one of the reasons why the present framework provides better results than the standard MFT.[25]

Expanding only the terms on the right-hand sides of Eqs. (7) and (10), one can obtain the following set of coupled equations for the layer magnetizations:

$$\begin{aligned}m_{\rm A} = {} & A_0+A_1m_{\rm A}+{\rm A}_2m_{\rm A}^2+A_3m_{\rm A}^3+A_4m_{\rm A}^4+A_5m_{\rm A}^5+A_6m_{\rm A}^6+A_7m_{\rm A}^7+A_8m_{\rm A}^8+A_9m_{\rm A}^9\\ &+A_{10}m_{\rm B}+A_{11}m_{\rm A}m_{\rm B}+A_{12}m_{\rm A}^2m_{\rm B}+A_{13}m_{\rm A}^3m_{\rm B}+A_{14}m_{\rm A}^4m_{\rm B}+A_{15}{\rm m}_{\rm A}^5m_{\rm B}+A_{16}m_{\rm A}^6m_{\rm B}\\ &+A_{17}m_{\rm A}^7m_{\rm B}+A_{18}m_{\rm A}^8m_{\rm B}+A_{19}m_{\rm A}^9m_{\rm B}+A_{20}m_{\rm B}^2+A_{21}m_{\rm A}m_{\rm B}^2+A_{22}m_{\rm A}^2m_{\rm B}^2+A_{23}m_{\rm A}^3m_{\rm B}^2\\ &+A_{24}m_{\rm A}^4m_{\rm B}^2+A_{25}m_{\rm A}^5m_{\rm B}^2+A_{26}m_{\rm A}^6m_{\rm B}^2+A_{27}m_{\rm A}^7m_{\rm B}^2+A_{28}m_{\rm A}^8m_{\rm B}^2+A_{29}m_{\rm A}^9m_{\rm B}^2\\ &+A_{30}m_{\rm B}^3+A_{31}{\rm m}_{\rm A}m_{\rm B}^3+A_{32}m_{\rm A}^2m_{\rm B}^3+A_{33}m_{\rm A}^3m_{\rm B}^3+A_{34}m_{\rm A}^4m_{\rm B}^3+A_{35}m_{\rm A}^5{\rm m}_{\rm B}^3+A_{36}m_{\rm A}^6m_{\rm B}^3\\ &+A_{37}m_{\rm A}^7m_{\rm B}^3+A_{38}m_{\rm A}^8m_{\rm B}^3+A_{39}m_{\rm A}^9m_{\rm B}^3+A_{40}m_{\rm B}^4+A_{41}m_{\rm A}m_{\rm B}^4+A_{42}m_{\rm A}^2{\rm m}_{\rm B}^4+A_{43}m_{\rm A}^3m_{\rm B}^4\\ &+A_{44}m_{\rm A}^4m_{\rm B}^4+A_{45}m_{\rm A}^5m_{\rm B}^4+A_{46}m_{\rm A}^6m_{\rm B}^4+A_{47}m_{\rm A}^7m_{\rm B}^4+A_{48}m_{\rm A}^8m_{\rm B}^4+A_{49}m_{\rm A}^9m_{\rm B}^4+A_{50}m_{\rm B}^5\\ &+A_{51}m_{\rm A}m_{\rm B}^5+A_{52}m_{\rm A}^2m_{\rm B}^5+A_{53}m_{\rm A}^3m_{\rm B}^5+A_{54}m_{\rm A}^4m_{\rm B}^5+A_{55}m_{\rm A}^5m_{\rm B}^5+A_{56}m_{\rm A}^6m_{\rm B}^5+A_{57}m_{\rm A}^7m_{\rm B}^5\end{aligned}$$

$$
\begin{aligned}
&+A_{58}m_{\rm A}^{8}m_{\rm B}^{5}+{\rm A}_{59}m_{\rm A}^{9}m_{\rm B}^{5}+A_{60}m_{\rm B}^{6}+A_{61}m_{\rm A}m_{\rm B}^{6}+A_{62}m_{\rm A}^{2}{\rm m}_{\rm B}^{6}+A_{63}m_{\rm A}^{3}m_{\rm B}^{6}+A_{64}m_{\rm A}^{4}m_{\rm B}^{6}\\
&+A_{65}m_{\rm A}^{5}m_{\rm B}^{6}+A_{66}m_{\rm A}^{6}m_{\rm B}^{6}+A_{67}m_{\rm A}^{7}m_{\rm B}^{6}+A_{68}m_{\rm A}^{8}m_{\rm B}^{6}+A_{69}m_{\rm A}^{9}m_{\rm B}^{6}+A_{70}m_{\rm B}^{7}+A_{71}m_{\rm A}m_{\rm B}^{7}\\
&+A_{72}m_{\rm A}^{2}m_{\rm B}^{7}+A_{73}m_{\rm A}^{3}m_{\rm B}^{7}+A_{74}m_{\rm A}^{4}m_{\rm B}^{7}+A_{75}m_{\rm A}^{5}m_{\rm B}^{7}+A_{76}m_{\rm A}^{6}m_{\rm B}^{7}+A_{77}m_{\rm A}^{7}m_{\rm B}^{7}+A_{78}m_{\rm A}^{8}m_{\rm B}^{7}\\
&+A_{79}m_{\rm A}^{9}m_{\rm B}^{7}+A_{80}m_{\rm B}^{8}+A_{81}m_{\rm A}m_{\rm B}^{8}+A_{82}m_{\rm A}^{2}{\rm m}_{\rm B}^{8}+A_{83}m_{\rm A}^{3}m_{\rm B}^{8}+A_{84}m_{\rm A}^{4}m_{\rm B}^{8}+A_{85}m_{\rm A}^{5}m_{\rm B}^{8}\\
&+A_{86}m_{\rm A}^{6}m_{\rm B}^{8}+A_{87}m_{\rm A}^{7}m_{\rm B}^{8}+A_{88}m_{\rm A}^{8}m_{\rm B}^{8}+A_{89}m_{\rm A}^{9}m_{\rm B}^{8}, \qquad (14)\\
m_{\rm B}=&B_0+B_1m_{\rm A}+B_2m_{\rm A}^{2}+B_3m_{\rm A}^{3}+B_4m_{\rm A}^{4}+B_5m_{\rm A}^{5}+B_6m_{\rm A}^{6}+B_7{\rm m}_{\rm B}+B_8m_{\rm A}m_{\rm B}+B_9m_{\rm A}^{2}m_{\rm B}\\
&+B_{10}m_{\rm A}^{3}m_{\rm B}+B_{11}m_{\rm A}^{4}m_{\rm B}+B_{12}m_{\rm A}^{5}m_{\rm B}+B_{13}m_{\rm A}^{6}m_{\rm B}+B_{14}m_{\rm B}^{2}+B_{15}m_{\rm A}m_{\rm B}^{2}+B_{16}m_{\rm A}^{2}m_{\rm B}^{2}\\
&+B_{17}m_{\rm A}^{3}m_{\rm B}^{2}+B_{18}m_{\rm A}^{4}m_{\rm B}^{2}+B_{19}m_{\rm A}^{5}m_{\rm B}^{2}+B_{20}m_{\rm A}^{6}m_{\rm B}^{2}+B_{21}m_{\rm B}^{3}+B_{22}m_{\rm A}m_{\rm B}^{3}+B_{23}m_{\rm A}^{2}{\rm m}_{\rm B}^{3}\\
&+B_{24}m_{\rm A}^{3}m_{\rm B}^{3}+B_{25}m_{\rm A}^{4}m_{\rm B}^{3}+B_{26}m_{\rm A}^{5}m_{\rm B}^{3}+B_{27}m_{\rm A}^{6}m_{\rm B}^{3}+B_{28}m_{\rm B}^{4}+B_{29}m_{\rm A}m_{\rm B}^{4}+B_{30}m_{\rm A}^{2}{\rm m}_{\rm B}^{4}\\
&+B_{31}m_{\rm A}^{3}m_{\rm B}^{4}+B_{32}m_{\rm A}^{4}m_{\rm B}^{4}+B_{33}m_{\rm A}^{5}m_{\rm B}^{4}+B_{34}m_{\rm A}^{6}m_{\rm B}^{4}+B_{35}m_{\rm B}^{5}+B_{36}m_{\rm A}m_{\rm B}^{5}+B_{37}m_{\rm A}^{2}{\rm m}_{\rm B}^{5}\\
&+B_{38}m_{\rm A}^{3}m_{\rm B}^{5}+B_{39}m_{\rm A}^{4}m_{\rm B}^{5}+B_{40}m_{\rm A}^{5}m_{\rm B}^{5}+B_{41}m_{\rm A}^{6}m_{\rm B}^{5}+B_{42}m_{\rm B}^{6}+B_{43}m_{\rm A}m_{\rm B}^{6}+B_{44}m_{\rm A}^{2}{\rm m}_{\rm B}^{6}\\
&+B_{45}m_{\rm A}^{3}m_{\rm B}^{6}+B_{46}m_{\rm A}^{4}m_{\rm B}^{6}+B_{47}m_{\rm A}^{5}m_{\rm B}^{6}+B_{48}m_{\rm A}^{6}m_{\rm B}^{6}+B_{49}m_{\rm B}^{7}+B_{50}m_{\rm A}m_{\rm B}^{7}+B_{51}m_{\rm A}^{2}{\rm m}_{\rm B}^{7}\\
&+B_{52}m_{\rm A}^{3}m_{\rm B}^{7}+B_{53}m_{\rm A}^{4}m_{\rm B}^{7}+B_{54}m_{\rm A}^{5}m_{\rm B}^{7}+B_{55}m_{\rm A}^{6}m_{\rm B}^{7}+B_{56}m_{\rm B}^{8}+B_{57}m_{\rm A}m_{\rm B}^{8}+B_{58}m_{\rm A}^{2}{\rm m}_{\rm B}^{8}\\
&+B_{59}m_{\rm A}^{3}m_{\rm B}^{8}+B_{60}m_{\rm A}^{4}m_{\rm B}^{8}+B_{61}m_{\rm A}^{5}m_{\rm B}^{8}+B_{62}m_{\rm A}^{6}m_{\rm B}^{8}+B_{63}m_{\rm B}^{9}+B_{64}m_{\rm A}m_{\rm B}^{9}+B_{65}m_{\rm A}^{2}{\rm m}_{\rm B}^{9}\\
&+B_{66}m_{\rm A}^{3}m_{\rm B}^{9}+B_{67}m_{\rm A}^{4}m_{\rm B}^{9}+B_{68}m_{\rm A}^{5}m_{\rm B}^{9}+B_{69}m_{\rm A}^{6}m_{\rm B}^{9}+B_{70}m_{\rm B}^{10}+B_{71}m_{\rm A}m_{\rm B}^{10}+B_{72}m_{\rm A}^{2}m_{\rm B}^{10}\\
&+B_{73}m_{\rm A}^{3}m_{\rm B}^{10}+B_{74}m_{\rm A}^{4}m_{\rm B}^{10}+B_{75}m_{\rm A}^{5}m_{\rm B}^{10}+B_{76}m_{\rm A}^{6}m_{\rm B}^{10}+B_{77}m_{\rm B}^{11}+B_{78}m_{\rm A}m_{\rm B}^{11}+B_{79}m_{\rm A}^{2}m_{\rm B}^{11}\\
&+B_{80}m_{\rm A}^{3}m_{\rm B}^{11}+B_{81}m_{\rm A}^{4}m_{\rm B}^{11}+B_{82}m_{\rm A}^{5}m_{\rm B}^{11}+B_{83}m_{\rm A}^{6}m_{\rm B}^{11}+B_{84}m_{\rm B}^{12}+B_{85}m_{\rm A}m_{\rm B}^{12}+B_{86}m_{\rm A}^{2}m_{\rm B}^{12}\\
&+B_{87}m_{\rm A}^{3}m_{\rm B}^{12}+B_{88}m_{\rm A}^{4}m_{\rm B}^{12}+B_{89}m_{\rm A}^{5}m_{\rm B}^{12}+B_{90}m_{\rm A}^{6}m_{\rm B}^{12}, \qquad (15)
\end{aligned}
$$

where the coefficients A_i $(i = 0, 1, \ldots, 89)$ and B_j $(j = 0, 1, \ldots, 90)$ are calculated by using mathematical relations $\exp(\alpha\,\nabla)\,f(x) = f(x+\alpha)$ and $\exp(\alpha\,\nabla)\,g(x) = g(x+\alpha)$ and given in Appendix B. Solving the coupled equations (14) and (15), we can obtain the layer magnetization curves. We will perform this calculation in the next section.

On the other hand, the average total magnetization of the system is given by

$$m_{\rm T} = (m_{\rm A} \pm m_{\rm B})/2. \qquad (16)$$

The average total magnetization ($m_{\rm T}$) vanishes at the compensation temperature $T_{\rm comp}$. The compensation point then, can be determined by looking for the crossing point between the absolute values of the sublattice magnetizations. Therefore, at the compensation point, we must have

$$|m_{\rm A}(T_{\rm comp})| = |m_{\rm B}(T_{\rm comp})|, \qquad (17)$$

and

$$\mathrm{sgn}\,[m_{\rm A}(T_{\rm comp})] = -\mathrm{sgn}\,[m_{\rm B}(T_{\rm comp})]. \qquad (18)$$

We also require that $T_{\rm comp} < T_{\rm C}$, where $T_{\rm C}$ is the critical temperature.

The order parameters determing the different phases of the mixed spin-3/2 and spin-2 Ising system at zero temperature are given as follows:

(i) The paramagnetic phase (p): $m_{\rm A} = m_{\rm B} = 0$.

(ii) The ferrimagnetic phase (i): $m_{\rm A} \neq m_{\rm B} \neq 0$,

a) The ferrimagnetic (3/2, 2) phase (i_1): $m_{\rm A} = 3/2$, $m_{\rm B} = 2$;

b) The ferrimagnetic (–3/2, 2) phase (i_2): $m_{\rm A} = -3/2$, $m_{\rm B} = 2$;

c) The ferrimagnetic (3/2, 1) phase (i_3): $m_{\rm A} = 3/2$, $m_{\rm B} = 1$;

d) The ferrimagnetic (1/2, 2) phase (i_4): $m_{\rm A} = 1/2$, $m_{\rm B} = 2$;

e) The ferrimagnetic (1/2, 1) phase (i_5): $m_{\rm A} = 1/2$, $m_{\rm B} = 1$.

(iii) The non-magnetic phase (nm): $m_{\rm A} \neq 0$, $m_{\rm B} = 0$.

The similar phase definitions have been also used by various researchers, see Refs. [26]–[28].

3. Numerical results and discussion

In this section, we examine some interesting and typical results for the mixed spin-3/2 and spin-2 Ising system with alternative layers with a crystal–field in a longitudinal magnetic field. Since the zero temperature phase diagram can be exactly obtained and it

can be used to check the reliability of the theoretical results, we start our investigation by calculating the zero temperature phase diagram. The zero temperature phase diagram is obtained in the h/z_2J_{ab} versus Δ/z_2J_{ab} plane for $J_a = 2.0$, $J_b = J_{ab} = 1.0$ from the condition of the values of the minimum energy of the configuration by comparing with the energies of the other configuration for a given set of the parameters as seen in Fig. 2. Each one of these configurations for the given system parameters corresponds to the stable state of the model. Hence, we have eight possible spin configurations for $J_a = 2.0$, $J_b = J_{ab} = 1.0$. All possible spin configurations are also indicated in the ground-state phase diagram as seen in Fig. 2. It has three multicritical points where more than one phase can coexist, namely A_1, A_2, and A_3.

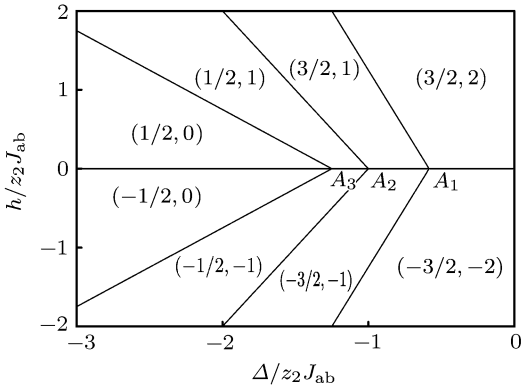


Fig. 2. Zero temperature phase diagram of the mixed spin-3/2 and spin-2 Ising system with alternative layers in the (Δ/z_2J_{ab}, h/z_2J_{ab}) plane for $J_a = 2.0$, $J_b = J_{ab} = 1.0$. A_1, A_2, and A_3 are the multicritical points where more than one phase can coexist.

We investigate the thermal behaviours of layer magnetizations (m_A and m_B) on the honeycomb lattice by solving Eqs. (14) and (15) numerically and as a result, the nature (continuity and discontinuity) of transitions can be obtained. After the detailed investigations of the behaviour of layer magnetizations, we present the phase diagrams in seven different planes. Figure 3(a) shows the thermal behaviours of layer magnetizations for $J_b/J_a = 0.1$, $z_2J_{ab}/z_1J_a = 0.66$, and $\Delta/z_1J_a = 0.33$. In this figure, $m_A = 3/2$ and $m_B = 2$ are at zero temperature and they decrease to zero continuously as the temperature increases; hence a second-order phase transition occurs at $kT/z_1J_a = 2.113$. The transition is from the ferrimagnetic-(3/2, 2) phase (i_1) to the paramagnetic phase (p). Figure 3(b) is obtained for the negative J_{ab}/J_a, i.e., $J_b/J_a = 0.1$ and $z_2J_{ab}/z_1J_a = -0.66$. In this case, $m_A = -3/2$ and $m_B = 2$ are at zero temperature and they go to zero continuously as the temperature increases, therefore a second-order phase transition also occurs at $kT/z_1J_a = 2.113$. The transition is from the ferrimagnetic-(−3/2, 2) phase (i_2) to the p phase. It can be seen from Figs. 3(a) and 3(b), changing the sign of J_{ab}/J_a does not affect the phase transition temperature. Actually, changing the sign of J_{ab}/J_a is compensated by changing only the sign of one of the magnetization values, i.e., m_A. Moreover, from the behaviour of the total magnetization, one compensation temperature or N-type behaviour occurs in the system that exhibits the same behaviour as that classified in the Néel theory[29] as the N-type behaviour.[30] Figure 3(c) is obtained for $z_2J_{ab}/z_1J_a = 0$ and $J_b/J_a = 0.1$. In this figure $m_A = 3/2$ and $m_B = 2$ are at zero temperature and m_B goes to zero continuously as the temperature increases; the transition occurs at $kT/z_1J_a = 0.376$. If the temperature increases further

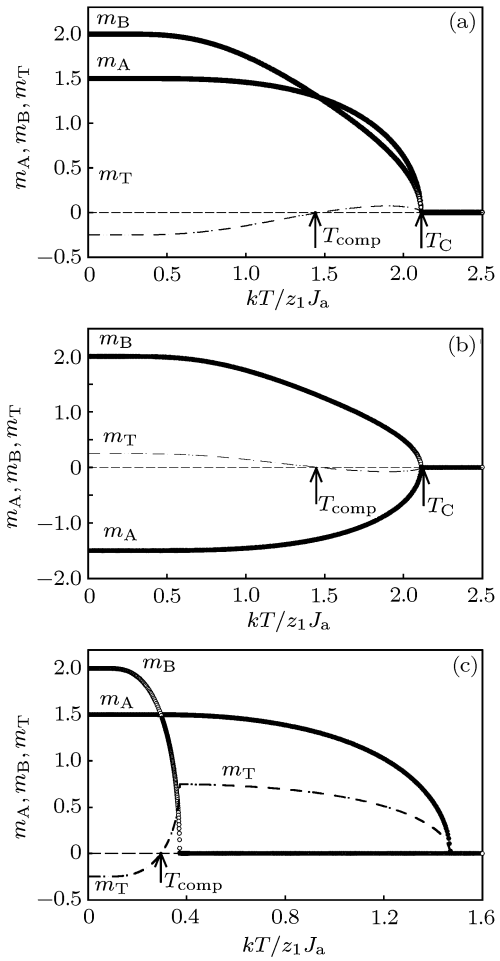


Fig. 3. Temperature dependences of the magnetizations of each layer m_A, m_B and m_T on honeycomb lattice for $J_b/J_a = 0.1$ and $z_2J_{ab}/z_1J_a = 0.66$ (a), $J_b/J_a = 0.1$ and $z_2J_{ab}/z_1J_a = -0.66$ (b), and $J_b/J_a = 0.1$ and $z_2J_{ab}/z_1J_a = 0.0$ (c).

$m_{\rm A}$ goes to zero continuously while $m_{\rm B}$ equals zero up to $kT/z_1J_{\rm a} = 1.476$. These transition points correspond to the isolated critical point (C_1) and multicritical point (A_1) shown by comparing Fig. 3(c) with Fig. 5(a).

We also investigate the behaviours of layer magnetizations as a function of the internal parameter $J_{\rm ab}/J_{\rm a}$ and present two representative graphs as seen in Fig. 4. Figure 4(a) is illustrated for the values of $J_{\rm b}/J_{\rm a} = 0.1$ and $kT/z_1J_{\rm a} = 2.0$. In Fig. 4(a), $m_{\rm A}$ starts from $-3/2$ and $m_{\rm B}$ starts from 2 for negative values of $J_{\rm ab}/J_{\rm a}$; hence we have the i_2 phase; as the internal parameter $J_{\rm ab}/J_{\rm a}$ increases, $m_{\rm B}$ decreases and $m_{\rm A}$ increases continuously and finally they become zero at $z_2J_{\rm ab}/z_1J_{\rm a} = -0.573$; hence the system undergoes a second-order phase transition and the transition is from the i_2 phase to the p phase. The p phase exists between the values of $z_2J_{\rm ab}/z_1J_{\rm a} = -0.573$ and $z_2J_{\rm ab}/z_1J_{\rm a} = 0.573$. As the internal parameter $J_{\rm ab}/J_{\rm a}$ increases further, the layer magnetizations start to increase at $z_2J_{\rm ab}/z_1J_{\rm a} = 0.573$ and finally $m_{\rm A}$ becomes $3/2$ and $m_{\rm B}$ becomes 2; hence, we have i_1 phase. Thus, the transition is from the p phase to the i_1 phase. Figure 4(b) shows a first-order phase transition and it is obtained for $J_{\rm b}/J_{\rm a} = 0.1$ and $kT/z_1J_{\rm a} = 0.33$. In this figure $m_{\rm A} = -3/2$ and $m_{\rm B}$=2 for negative values of internal parameter $J_{\rm ab}/J_{\rm a}$, then, as the $J_{\rm ab}/J_{\rm a}$ increases, $m_{\rm A}$ and $m_{\rm B}$ present a jump discontinuities at $z_2J_{\rm ab}/z_1J_{\rm a} = 0$. Then, as the internal parameter $J_{\rm ab}/J_{\rm a}$ increases $m_{\rm A}$ and $m_{\rm B}$ increase and they become $3/2$ and 2, respectively; hence the system undergoes a first-order phase transition from the i_2 phase to the i_1 phase. The system also exhibits two compensation points. Figure 4(c) is obtained for $J_{\rm b}/J_{\rm a} = 0.1$ and $kT/z_1J_{\rm a} = 0.833$. While figure 4(c) is the same as Fig. 4(b), but differs from Fig. 3(b) in which $m_{\rm B}$ goes to zero continuously and meets with zero at $z_2J_{\rm ab}/z_1J_{\rm a} = 0$; if $J_{\rm ab}/J_{\rm a}$ increases further $m_{\rm B}$ continuously increases and becomes 2. At this point, we should emphasize that within the present effective-field framework and based on the differential operator technique it is not possible to determine the first-order phase transitions because the complete function for the free energy has not obtained analytically. Therefore, we determine the first-order phase transition temperature as well as the first-order transition line to investigate the thermal behaviour of the order parameters. More precisely, if the order parameters decrease to zero discontinuously as the reduced temperature increases a first-order phase transition occurs. The first-order phase transition temperature is the temperature at which the discontinuity takes place.

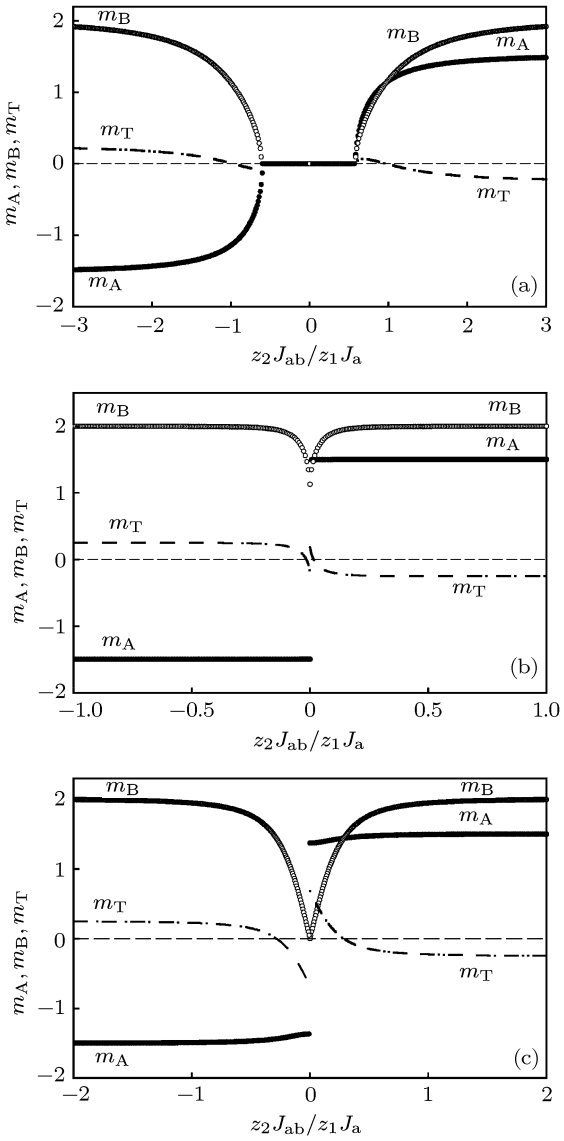


Fig. 4. Variations of the magnetizations of each layer $m_{\rm A}$, $m_{\rm B}$ and $m_{\rm T}$ with internal parameter $J_{\rm ab}/J_{\rm a}$ on the honeycomb lattice for $J_{\rm b}/J_{\rm a} = 0.1$ and $kT/z_1J_{\rm a} = 2.0$ (a), $J_{\rm b}/J_{\rm a} = 0.1$ and $kT/z_1J_{\rm a} = 0.33$ (b), and $J_{\rm b}/J_{\rm a} = 0.1$ and $kT/z_1J_{\rm a} = 0.833$ (c).

We are now ready to present the phase diagrams in the interaction parameters and the reduced temperature planes, namely ($kT/z_1J_{\rm a}$, $z_2J_{\rm ab}/z_1J_{\rm a}$), ($kT/z_2J_{\rm ab}$, $z_1J_{\rm a}/z_2J_{\rm ab}$), ($kT/z_2J_{\rm ab}$, $z_1J_{\rm b}/z_2J_{\rm ab}$), ($\Delta/z_2J_{\rm ab}$, $z_1J_{\rm a}/z_2J_{\rm ab}$), ($\Delta/z_2J_{\rm ab}$, $z_1J_{\rm b}/z_2J_{\rm ab}$), ($z_1J_{\rm a}/z_2J_{\rm ab}$, $kT/z_2J_{\rm ab}$), and ($z_1J_{\rm b}/z_2J_{\rm ab}$, $kT/z_2J_{\rm ab}$) planes for $h = 0$ as seen in Figs. 5, 6 and 7. Figure 5 expresses the finite temperature phase diagram in the ($kT/z_1J_{\rm a}$, $z_2J_{\rm ab}/z_1J_{\rm a}$) plane. In the figure, the solid, dashed and dash-dot-dot lines represent the second-,

first-order phase transition and compensation temperature lines, respectively. The open circles indicate the isolated critical points at which the first-order phase transition lines terminate along the $z_2J_{ab}/z_1J_a = 0.0$ and the solid circles denote the multicritical points. These points are labeled with C_i, $i = 1$, 2, 3, and 4 (isolated critical); and A_j, $j = 1$, 2, 3, and 4 (multicritical) for $J_b/J_a = 0.1$, 0.5, 1.0, and 2.0, respectively. Figure 5(a) is obtained for $J_b/J_a < 0.62$, namely $J_b/J_a = 0.1$ and 0.5. In the phase diagram, the phase boundary between the i_1 and i_2 phases is a first-order phase line for $0 \le kT/z_1J_a \le C_i$. The system does not undergo any phase transition for $C_i \le kT/J_a \le A_j$ where $m_A \neq 0$ and $m_B = 0$. For $kT/z_1J_a > A_j$, the system undergoes a second-order phase transition; hence the boundaries among the i_1, i_2, and p phases are second-order lines. These second-order lines are symmetrical wing-shape, as seen in Fig. 5. We should also mention that for $J_b/J_a \le 0.62A_j$ points occur at the same temperature, i.e, $A_1 = A_2$ as seen in the figure. Moreover, for $J_b/J_a = 0.62$ C_i and A_j points exist at the same temperature. Figure 5(b) is calculated for $J_b/J_a > 0.62$. This phase diagram is similar to that in Fig. 5(a), except that the C_i points occur at the same temperature instead of A_j points and the compensation temperatures disappear. Similar phase diagrams to Figs. 5(a) and 5(b) are also obtained in the mixed spins (1, 3/2) on the Bethe lattice,[14,31] the spin-1/2 Ising model on honeycomb and square lattices for alternative layers[32] and the mixed spin (1, 3/2) Ising system with two alternative layers of a honeycomb lattice[33] within the EFT. Moreover, the phase diagrams in Figs. 5(a) and 5(b) look similar to the one obtained for the bilayer Bethe lattices[34] using exact recursion relations and the Co/Cu/Ni trilayer system[35] by using the Green's function approach.

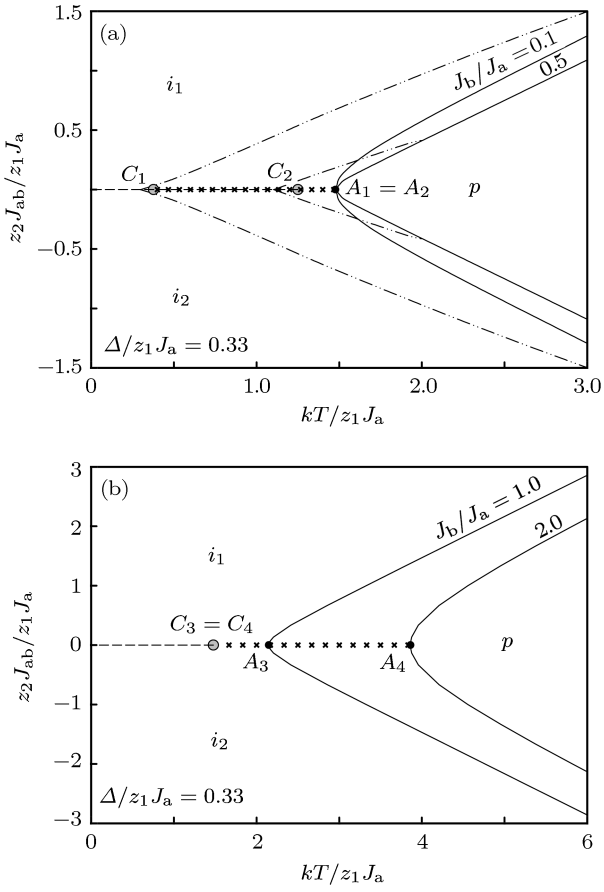


Fig. 5. Phase diagrams in the $(kT/z_1J_a, z_2J_{ab}/z_1J_a)$ plane for the Ising system with alternative layers on the honeycomb lattice. Solid, dashed and dash-dot-dot lines indicate the second-, first-order phase boundaries and compensation temperature lines, respectively; the isolated critical (C_i) and multicritical (A_j) points are marked with open and solid circles, respectively. The isolated critical points ($C_3 = C_4$) for $J_b/J_a = 1.0$ and 2.0 and the multicritical points ($A_1 = A_2$) for $J_b/J_a = 0.1$ and 0.5 occur at the same temperature. Internal parameters are J_b/J_a and J_{ab}/J_a which measure the strength of exchange interaction between intralayer and interlayer, respectively, for honeycomb lattice for $\Delta/z_1J_a = 0.33$, $J_b/J_a = 0.1$ and 0.5 (a), and $\Delta/z_1J_a = 0.33$, $J_b/J_a = 1.0$ and 2.0 (b).

The phase diagrams in Figs. 6(a) and 6(b) are obtained in the $(kT/z_2J_{ab}, z_1J_a/z_2J_{ab})$ and $(kT/z_2J_{ab}, z_1J_b/z_2J_{ab})$ planes for given values of J_b/J_{ab} and J_a/J_{ab}, respectively. As seen from the figures, the system always presents second-order phase transitions. The behaviours of the second-order phase transition lines are similar in both figures, in which they start from the lower kT/J_{ab} values for the lower values of J_a/J_{ab} (J_b/J_{ab}) when $z_1J_a/z_2J_{ab} = 0$ ($z_1J_b/z_2J_{ab} = 0$) and as kT/J_{ab} increases the second-order phase transition lines increase with respect to J_a/J_{ab} (J_b/J_{ab}) values as seen in Fig. 6(a) (Fig. 6(b)). In the end, they all combine and increase linearly. On the other hand, the behaviour of the compensation temperature, T_{comp}, lines are quite different; in Fig. 6(a) the T_{comp} lines start from the lower kT/z_2J_{ab} for lower values of J_a/J_{ab}, which correspond to T_C lines and as J_a/J_{ab} increases they make curves, a little bent towards the left side at lower temperatures and with the further increase in J_a/J_{ab}, finally these lines become constant; but in Fig. 6(b) all the T_{comp} lines emerge from the same $kT/z_2J_{ab} = 1.81$ when $z_1J_b/z_2J_{ab} = 0$, as J_b/J_{ab} increases their compensation temperatures increase and terminate on the corresponding second-order phase transition lines. Similar phase diagrams to Figs. 6(a) and 6(b) are also

obtained for bilayer model of spin-1 and spin-3/2 on the Bethe lattice[31] and the mixed spin (1, 3/2) Ising system with two alternative layers of a honeycomb lattice.[33]

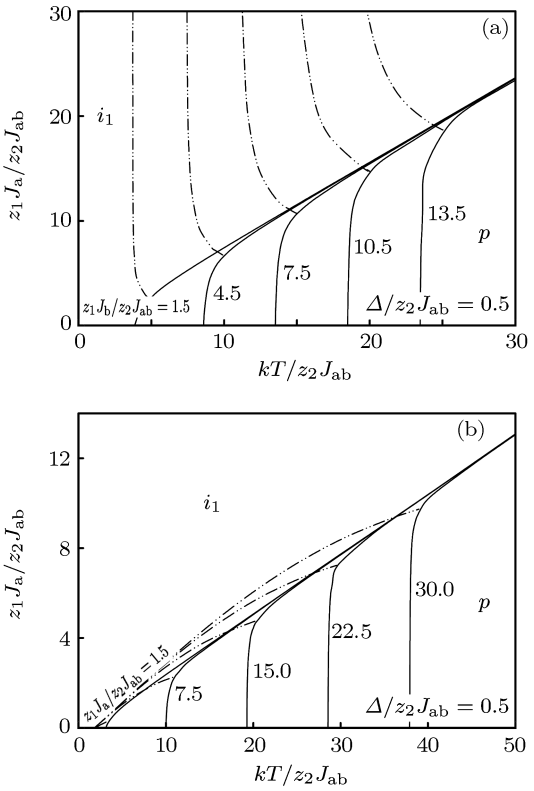


Fig. 6. Phase diagrams when $\Delta/z_2J_{ab} = 0.5$ on the (kT/z_2J_{ab}, z_1J_a/z_2J_{ab}) plane (a) and the (kT/z_2J_{ab}, z_1J_b/z_2J_{ab}) plane (b), showing the relation between the layers for compensation.

We also calculate the phase diagrams including the compensation behaviours in the (Δ/z_2J_{ab}, z_1J_a/z_2J_{ab}), (Δ/z_2J_{ab}, z_1J_b/z_2J_{ab}), (z_1J_a/z_2J_{ab}, kT/z_2J_{ab}), and (z_1J_b/z_2J_{ab}, kT/z_2J_{ab}) planes. From these phase diagrams the following interesting phenomena have been observed. (i) Figures 7(a) and 7(b) are obtained in the (Δ/z_2J_{ab}, z_1J_a/z_2J_{ab}) plane for $J_b = J_{ab} = 1.0$, $kT/z_2J_{ab} = 0.5$, and $kT/z_2J_{ab} = 2.5$, respectively. Figure 7(a) exhibits the i_1, i_3, nm, and p phases, besides the critical end point (E) and isolated critical point (C). The phase boundaries among these phases are first-order phase transition lines, except the negative high values of Δ/z_2J_{ab} that the phase boundary between the nm and p phases is the second-order phase transition line. The lines of the first-order phase transitions between the i_1 phase and the i_3 phase are found to end at the isolated critical point (C). The isolated critical point was also observed in the mean field solution of the general spin Blume–Capel model.[36] Moreover, this figure also exhibits a kind of reentrant behaviour for $-3.430 \leq \Delta/z_2J_{ab} \leq -3.165$; i.e., as the J_a increases, the system passes from the nm phase to the i_3 phase and then back to the nm phase again and finally passes to the i_3 phase. It also displays the compensation temperature in the i_1 phase. (ii) Figure 7(b) is constructed for $J_a = J_{ab} = 1.0$ and $kT/z_2J_{ab} = 0.5$ in the (Δ/z_2J_{ab}, z_1J_b/z_2J_{ab}) plane. The phase diagram exhibits the i_1, i_4, i_5, and p phases, besides the isolated critical point (C) and the triple point (TP) that merge three first-order phase transition lines. In this case, the system only undergoes a first-order phase transition and the first-order phase lines separate all phases from each other as seen in Fig. 7(b). In this case the system does not exhibit the compensation behaviour. (iii) For $J_b = J_{ab} = 1.0$ and $\Delta/z_2J_{ab} = 0.5$ the phase diagram is obtained in (z_1J_a/z_2J_{ab}, kT/z_2J_{ab}) plane; the system contains p and i_1 phases, the boundary between these phases is a second-order line as seen in Fig. 7(c). Moreover, the system also displays the compensation behaviour. (iv) Figure 7(d) is calculated in (z_1J_b/z_2J_{ab}, kT/z_2J_{ab}) plane for $z_1J_a/z_2J_{ab} = 1.33$, $z_2J_{ab} = 0.5$, $\Delta/z_2J_{ab} = 0.5$, respectively. In this figure, the system always undergoes a second-order phase transition which separates the p phase from the i_1 phase and it also exhibits the compensation behaviour. We should also mention that for low values of J_a the phase diagram in this plane does not display the compensation behaviour. We have also found a similar behaviour to Figs. 7(c) and 7(d) to the one seen in the previous studies.[33,37–40]

In summary, we have studied the magnetization curves and phase diagrams of the mixed spin-3/2 and spin-2 Ising system with alternative layers on the honeycomb lattice within the framework of the effective-field theory (EFT) with correlations. It is assumed that while the intralayer coupling constants of the layers are J_a and J_b and they are taken to be positive, the interlayer coupling constant between the layers is J_{ab} and it is taken to be either positive or negative. We have investigated the temperature dependence of the layer magnetizations to obtain the phase transition points as well as to characterize the nature (continuity or discontinuity) of transitions. The behaviour of the layer magnetization as a function of internal parameter (z_2J_{ab}/z_1J_a), which is the mixing ratio between interlayer couplings, is also presented. In order to find the compensation temperatures and to determine the type of behaviour, the total magnetization is examined as a function of temperature. From the behaviour

of the total magnetization, one can see that N-type compensation temperature occurs in the system.[29,30] The phase diagrams are constructed in seven different planes and it is found that the system also presents the compensation phenomenon depending on the sign of the bilinear exchange interaction. The obtained phase diagrams are constructed in seven different planes, namely (kT/z_1J_a, z_2J_{ab}/z_1J_a), (kT/z_2J_{ab}, z_1J_a/z_2J_{ab}), (kT/z_2J_{ab}, z_1J_b/z_2J_{ab}), (Δ/z_2J_{ab}, z_1J_a/z_2J_{ab}), (Δ/z_2J_{ab}, z_1J_b/z_2J_{ab}), (z_1J_a/z_2J_{ab}, kT/z_2J_{ab}), and (z_1J_b/z_2J_{ab}, kT/z_2J_{ab}) planes. The system exhibits both second- and first-order phase transitions besides triple point (TP), critical end point (E), multicritical point (A), isolated critical point (C), and reentrant behaviour, which depend on the interaction parameters. We should also mention that the phase diagrams obtained in the present study look similar to those obtained in the mixed spins (1, 3/2) on the Bethe lattice,[14,31] the spin-1/2 Ising model on honeycomb and square lattices for three alternative layers,[32] the mixed spin (1, 3/2) Ising system with two alternative layers of a honeycomb lattice[33] within the EFT, the bilayer Bethe lattice[34] by using the exact recursion relations and the Co/Cu/Ni trilayer system[35] using Green's function approach. Finally, we expect this work to stimulate further experimental and theoretical investigations and also help technological researches.

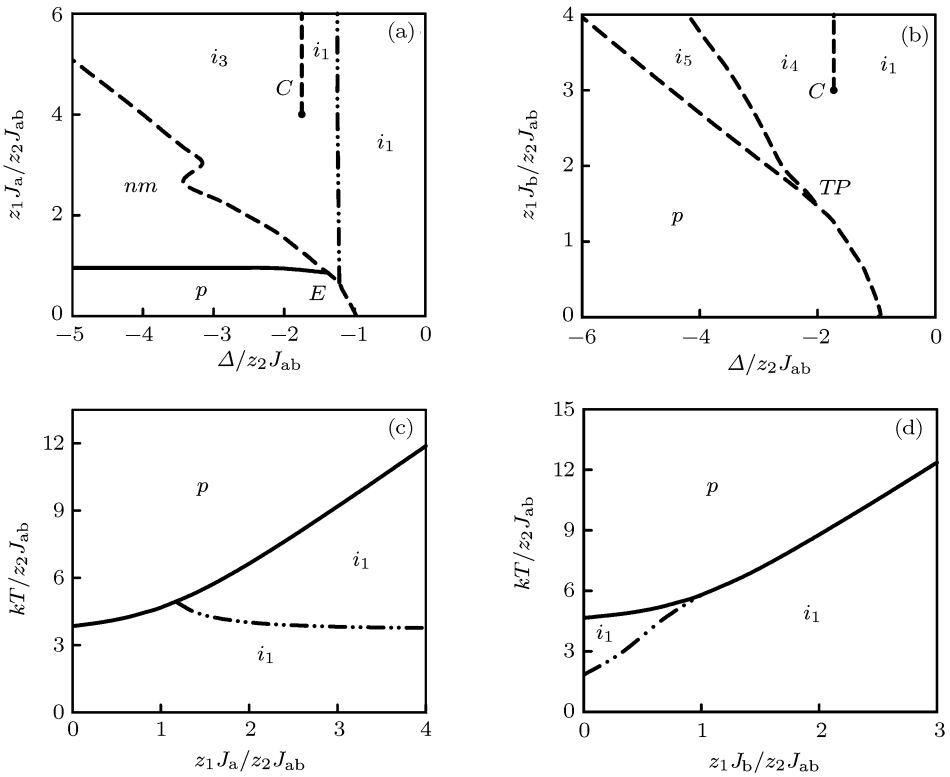


Fig. 7. Phase diagrams of the mixed spin-3/2 and spin-2 Ising system in the (Δ/z_2J_{ab}, z_1J_a/z_2J_{ab}), (Δ/z_2J_{ab}, z_1J_b/z_2J_{ab}), (z_1J_a/z_2J_{ab}, kT/z_2J_{ab}), and (z_1J_b/z_2J_{ab}, kT/z_2J_{ab}) planes. Dashed and solid lines are the first- and second-order phase boundaries, respectively. The dash–dot–dot line illustrates the compensation temperatures in (Δ/z_2J_{ab}, z_1J_a/z_2J_{ab}) plane for $J_b = J_{ab} = 1.0$, $kT/z_2J_{ab} = 0.5$ (a), (Δ/z_2J_{ab}, z_1J_b/z_2J_{ab}) plane for $J_a = J_{ab} = 1.0$ and $kT/z_2J_{ab} = 0.5$ (b), (z_1J_a/z_2J_{ab}, kT/z_2J_{ab}) plane for $J_b = J_{ab} = 1.0$ and $\Delta/z_2J_{ab} = 0.5$ (c), and (z_1J_b/z_2J_{ab}, kT/z_2J_{ab}) plane for $z_1J_a = 0.66$, $z_2J_{ab} = 0.5$, and $\Delta/z_2J_{ab} = 0.5$ (d).

Appendix A

The coefficients $A(J_a\nabla), B(J_a\nabla), C(J_a\nabla), D(J_a\nabla)$, and $A(J_{ab}\nabla), B(J_{ab}\nabla), C(J_{ab}\nabla), D(J_{ab}\nabla)$ for spin-3/2, and $K(J_b\nabla), L(J_b\nabla), M(J_b\nabla), N(J_b\nabla)$, and $K(J_{ab}\nabla), L(J_{ab}\nabla), M(J_{ab}\nabla), N(J_{ab}\nabla)$ for spin-2 in Eqs. (2) and (3), are defined as follows:

$$A(J_{\rm a}\nabla)=\frac{1}{8}\left[9\cosh\left(\frac{J_{\rm a}\nabla}{2}\right)-\cosh\left(\frac{3J_{\rm a}\nabla}{2}\right)\right],$$
$$A(J_{\rm ab}\nabla)=\frac{1}{8}\left[9\cosh\left(\frac{J_{\rm ab}\nabla}{2}\right)-\cosh\left(\frac{3J_{\rm ab}\nabla}{2}\right)\right],$$
$$B(J_{\rm a}\nabla)=\frac{1}{12}\left[27\sinh\left(\frac{J_{\rm a}\nabla}{2}\right)-\sinh\left(\frac{3J_{\rm a}\nabla}{2}\right)\right],$$
$$B(J_{\rm ab}\nabla)=\frac{1}{12}\left[27\sinh\left(\frac{J_{\rm ab}\nabla}{2}\right)-\sinh\left(\frac{3J_{\rm ab}\nabla}{2}\right)\right],$$
$$C(J_{\rm a}\nabla)=\frac{1}{2}\left[-\cosh\left(\frac{J_{\rm a}\nabla}{2}\right)+\cosh\left(\frac{3J_{\rm a}\nabla}{2}\right)\right],$$
$$C(J_{\rm ab}\nabla)=\frac{1}{2}\left[-\cosh\left(\frac{J_{\rm ab}\nabla}{2}\right)+\cosh\left(\frac{3J_{\rm ab}\nabla}{2}\right)\right],$$
$$D(J_{\rm a}\nabla)=\frac{1}{3}\left[-3\sinh\left(\frac{J_{\rm a}\nabla}{2}\right)+\sinh\left(\frac{3J_{\rm a}\nabla}{2}\right)\right],$$
$$D(J_{\rm ab}\nabla)=\frac{1}{3}\left[-3\sinh\left(\frac{J_{\rm ab}\nabla}{2}\right)+\sinh\left(\frac{3J_{\rm ab}\nabla}{2}\right)\right],$$
$$K(J_{\rm b}\nabla)=\frac{1}{6}\left[8\sinh(J_{\rm b}\nabla)-2\sinh(2J_{\rm b}\nabla)\right],$$
$$K(J_{\rm ab}\nabla)=\frac{1}{6}\left[8\sinh(J_{\rm ab}\nabla)-2\sinh(2J_{\rm ab}\nabla)\right],$$
$$L(J_{\rm b}\nabla)=\frac{1}{12}\left[16\cosh(J_{\rm b}\nabla)-\cosh(2J_{\rm b}\nabla)-15\right],$$
$$L(J_{\rm ab}\nabla)=\frac{1}{12}\left[16\cosh(J_{\rm ab}\nabla)-\cosh(2J_{\rm ab}\nabla)-15\right],$$
$$M(J_{\rm b}\nabla)=\frac{1}{6}\left[\sinh(2J_{\rm b}\nabla)-2\sinh(J_{\rm b}\nabla)\right],$$
$$M(J_{\rm ab}\nabla)=\frac{1}{6}\left[\sinh(2J_{\rm ab}\nabla)-2\sinh(J_{\rm ab}\nabla)\right],$$
$$N(J_{\rm b}\nabla)=\frac{1}{12}\left[\cosh(2J_{\rm b}\nabla)-4\cosh(J_{\rm b}\nabla)+3\right],$$
$$N(J_{\rm ab}\nabla)=\frac{1}{12}\left[\cosh(2J_{\rm ab}\nabla)-4\cosh(J_{\rm ab}\nabla)+3\right].$$

Appendix B

The coefficients A_i ($i=0,\ 1,\ \ldots,\ 89$) and B_j ($j=0,\ 1,\ \ldots,\ 90$) in Eqs. (14) and (15) are defined as follows:

$$\begin{aligned}
A_0 =& -\frac{1}{4096}[f(-9J_{\rm a}/2)-27f(-7J_{\rm a}/2)+216f(-5J_{\rm a}/2)-240f(-3J_{\rm a}/2)-1998f(-J_{\rm a}/2)\\
&-1998f(J_{\rm a}/2)-240f(-3J_{\rm a}/2)+216f(5J_{\rm a}/2)-27f(7J_{\rm a}/2)+f(9J_{\rm a}/2)],\\
&\vdots\\
A_{89} =& \frac{1}{124416}[-70f(-9J_{\rm a}/2)+630f(-7J_{\rm a}/2)-2520f(-5J_{\rm a}/2)+5880f(-3J_{\rm a}/2)-8820f(-J_{\rm a}/2)\\
&+8820f(J_{\rm a}/2)-5880f(3J_{\rm a}/2)+2520f(5J_{\rm a}/2)-630f(7J_{\rm a}/2)+70f(9J_{\rm a}/2)\\
&-f(-(9J_{\rm a}/2)-4J_{\rm ab})+9f(-(7{\rm J_a}/2)-4J_{\rm ab})-36{\rm f}(-(5J_{\rm a}/2)-4J_{\rm ab})-84f(-(3J_{\rm a}/2)-4J_{\rm ab})\\
&-126f(-(J_{\rm a}/2)-4{\rm J_{ab}})+126f(J_{\rm a}/2-4J_{\rm ab})-84f(3J_{\rm a}/2-4J_{\rm ab})+36f(5\,J_{\rm a}/2-4J_{\rm ab})\\
&-9f(7J_{\rm a}/2-4J_{\rm ab})+f(9J_{\rm a}/2-4J_{\rm ab})+8f(-(9J_{\rm a}/2)-3J_{\rm ab})-72f(-7J_{\rm a}/2-3J_{\rm ab})\\
&+288f(-5J_{\rm a}/2-3J_{\rm ab})-672f(-3J_{\rm a}/2-3J_{\rm ab})+1008f(-J_{\rm a}/2-3J_{\rm ab})-1008f(J_{\rm a}/2-3J_{\rm ab})\\
&+672f(3J_{\rm a}/2-3J_{\rm ab})-288f(5J_{\rm a}/2-3J_{\rm ab})+72f(7J_{\rm a}/2-3J_{\rm ab})-8f(9J_{\rm a}/2-3J_{\rm ab})\\
&-28f(-9J_{\rm a}/2-2J_{\rm ab})+252f(-7J_{\rm a}/2-2J_{\rm ab})-1008f(-5J_{\rm a}/2-2J_{\rm ab})+2352f(-3J_{\rm a}/2-2J_{\rm ab})\\
&-3528f(-J_{\rm a}/2-2J_{\rm ab})+3528f(J_{\rm a}/2-2J_{\rm ab})-2352f(3J_{\rm a}/2-2J_{\rm ab})+1008f(5J_{\rm a}/2-2J_{\rm ab})\\
&-252f(7J_{\rm a}/2-2J_{\rm ab})+28f(9J_{\rm a}/2-2J_{\rm ab})+56f(-9J_{\rm a}/2-J_{\rm ab})-504f(-7J_{\rm a}/2-J_{\rm ab})\\
&+2016f(-5J_{\rm a}/2-J_{\rm ab})-4704f(-3J_{\rm a}/2-J_{\rm ab})+7056f(-J_{\rm a}/2-J_{\rm ab})-7056f(J_{\rm a}/2-J_{\rm ab})\\
&+4704f(3J_{\rm a}/2-J_{\rm ab})-2016f(5J_{\rm a}/2-J_{\rm ab})+504f(7J_{\rm a}/2-J_{\rm ab})-56f(9J_{\rm a}/2-J_{\rm ab})\\
&+56f(-9J_{\rm a}/2+J_{\rm ab})-504f(-7J_{\rm a}/2+J_{\rm ab})+2016f(-5J_{\rm a}/2+J_{\rm ab})-4704f(-3J_{\rm a}/2+J_{\rm ab})\\
&+7056f(-J_{\rm a}/2+J_{\rm ab})-7056f(J_{\rm a}/2+J_{\rm ab})+4704f(3J_{\rm a}/2+J_{\rm ab})-2016f(5J_{\rm a}/2+J_{\rm ab})\\
&+504f(7J_{\rm a}/2+J_{\rm ab})-56f(9J_{\rm a}/2+J_{\rm ab})-28f(-9J_{\rm a}/2+2J_{\rm ab})+252f(-7J_{\rm a}/2+2J_{\rm ab})\\
&-1008f(-5J_{\rm a}/2+2J_{\rm ab})-2352f(-3J_{\rm a}/2+2J_{\rm ab})-3528f(-J_{\rm a}/2+2J_{\rm ab})+3528f(J_{\rm a}/2+2J_{\rm ab})\\
&-2352f(3J_{\rm a}/2+2J_{\rm ab})+1008f(5J_{\rm a}/2+2J_{\rm ab})-252f(7J_{\rm a}/2+2J_{\rm ab})+28f(9J_{\rm a}/2+2J_{\rm ab})\\
&+8f(-9J_{\rm a}/2+3J_{\rm ab})-72f(-7J_{\rm a}/2+3J_{\rm ab})+288f(-5J_{\rm a}/2+3J_{\rm ab})+672f(-3J_{\rm a}/2+3J_{\rm ab})\\
&+1008f(-J_{\rm a}/2+3J_{\rm ab})-1008f(J_{\rm a}/2+3J_{\rm ab})+672f(3J_{\rm a}/2+3J_{\rm ab})-288f(5J_{\rm a}/2+3J_{\rm ab})\\
&+72f(7J_{\rm a}/2+3J_{\rm ab})-8f(9J_{\rm a}/2+3J_{\rm ab})-f(-9J_{\rm a}/2+4J_{\rm ab})+9f(-7J_{\rm a}/2+4J_{\rm ab})\\
&-36f(-5J_{\rm a}/2+4J_{\rm ab})+84f(-3J_{\rm a}/2+4J_{\rm ab})-126f(-J_{\rm a}/2+4J_{\rm ab})+126f(J_{\rm a}/2+4J_{\rm ab})
\end{aligned}$$

$$
\begin{aligned}
&- 84f(3J_{\rm a}/2+4J_{\rm ab})+36{\rm f}(5J_{\rm a}/2+4J_{\rm ab})-9f(7J_{\rm a}/2+4J_{\rm ab})+f(9J_{\rm a}/2+4J_{\rm ab})],\\
B_0 &= \frac{1}{256}[164g(0)+g(-3J_{\rm ab})-18{\rm g}(-2J_{\rm ab})+63g(-J_{\rm ab})+63g(J_{\rm ab})-18{\rm g}(2J_{\rm ab})+g(3J_{\rm ab})],\\
B_{90} &= \frac{1}{497664}[-18480g(0)-20g(-6J_{\rm b})+240g(-5J_{\rm b})-1320g(-4J_{\rm b})+4400g(-3J_{\rm b})\\
&- 9900g(-2J_{\rm b})+15840g(-J_{\rm b})+15840g(J_{\rm b})-9900g(2J_{\rm b})+4400g(3J_{\rm b})\\
&- 1320g(4J_{\rm b})+240g(5J_{\rm b})-20g(6J_{\rm b})+924g(-3J_{\rm ab})-5544g(-2J_{\rm ab})+13860g(-J_{\rm ab})\\
&+ 13860g(J_{\rm ab})-5544g(2J_{\rm ab})+924g(3J_{\rm ab})+g(-6J_{\rm b}-3J_{\rm ab})-12g(-5J_{\rm b}-3J_{\rm ab})\\
&+ 66g(-4J_{\rm b}-3J_{\rm ab})-220{\rm g}(-3J_b-3J_{\rm ab})+495g(-2J_{\rm b}-3J_{\rm ab})-792g(-J_{\rm b}-3J_{\rm ab})\\
&- 792g(J_{\rm b}-3J_{\rm ab})+495g(2J_{\rm b}-3J_{\rm ab})-220g(3J_{\rm b}-3J_{\rm ab})+66g(4J_{\rm b}-3J_{\rm ab})\\
&- 12g(5J_{\rm b}-3J_{\rm ab})+{\rm g}(6J_{\rm b}-3J_{\rm ab})-6g(-6J_{\rm b}-2J_{\rm ab})+72g(-5J_{\rm b}-2J_{\rm ab})\\
&- 396g(-4J_{\rm b}-2J_{\rm ab})+1320{\rm g}(-3J_{\rm b}-2J_{\rm ab})-2970g(-2J_{\rm b}-2J_{\rm ab})+4752g(-J_{\rm b}-2J_{\rm ab})\\
&+ 4752g(J_{\rm b}-2J_{\rm ab})-2970{\rm g}(2J_{\rm b}-2J_{\rm ab})+1320g(3J_{\rm b}-2J_{\rm ab})-396g(4J_{\rm b}-2J_{\rm ab})\\
&+ 72g(5J_{\rm b}-2J_{\rm ab})-6{\rm g}(6J_{\rm b}-2J_{\rm ab})+15g(-6J_{\rm b}-J_{\rm ab})-180g(-5J_{\rm b}-J_{\rm ab})\\
&+ 990g(-4J_{\rm b}-J_{\rm ab})-3300{\rm g}(-3J_{\rm b}-J_{\rm ab})+7425g(-2J_{\rm b}-J_{\rm ab})-11880g(-J_{\rm b}-J_{\rm ab})\\
&- 11880g(J_{\rm b}-J_{\rm ab})+7425g(2J_{\rm b}-J_{\rm ab})-3300g(3J_{\rm b}-J_{\rm ab})+990g(4J_{\rm b}-J_{\rm ab})\\
&- 180g(5J_{\rm b}-J_{\rm ab})+15g(6J_{\rm b}-J_{\rm ab})+15g(-6J_{\rm b}+J_{\rm ab})-180g(-5J_{\rm b}+J_{\rm ab})\\
&+ 990g(-4J_{\rm b}+J_{\rm ab})-3300{\rm g}(-3J_{\rm b}+J_{\rm ab})+7425g(-2J_{\rm b}+J_{\rm ab})-11880g(-J_{\rm b}+J_{\rm ab})\\
&- 11880g(J_{\rm b}+J_{\rm ab})+7425g(2J_{\rm b}+J_{\rm ab})-3300g(3J_{\rm b}+J_{\rm ab})+990g(4J_{\rm b}+J_{\rm ab})\\
&- 180g(5J_{\rm b}+J_{\rm ab})+15g(6J_{\rm b}+J_{\rm ab})-6g(-6J_{\rm b}+2J_{\rm ab})+72g(-5J_{\rm b}+2J_{\rm ab})\\
&- 396g(-4J_{\rm b}+2J_{\rm ab})+1320{\rm g}(-3{\rm J}_{\rm b}+2J_{\rm ab})-2970g(-2J_{\rm b}+2J_{\rm ab})+4752g(-J_{\rm b}+2J_{\rm ab})\\
&+ 4752g(J_{\rm b}+2J_{\rm ab})-2970g(2J_{\rm b}+2J_{\rm ab})+1320g(3J_{\rm b}+2J_{\rm ab})-396g(4J_{\rm b}+2J_{\rm ab})\\
&+ 72g(5J_{\rm b}+2J_{\rm ab})-6{\rm g}(6J_{\rm b}+2J_{\rm ab})+g(-6J_{\rm b}+3J_{\rm ab})-12g(-5J_{\rm b}+3J_{\rm ab})\\
&+ 66g(-4J_{\rm b}+3J_{\rm ab})-220g(-3J_{\rm b}+3J_{\rm ab})+495g(-2J_b+3J_{\rm ab})-792g(-J_{\rm b}+3J_{\rm ab})\\
&- 792g(J_{\rm b}+3J_{\rm ab})+495g(2J_{\rm b}+3J_{\rm ab})-220g(3J_{\rm b}+3J_{\rm ab})+66g(4J_{\rm b}+3J_{\rm ab})\\
&- 12g(5J_{\rm b}+3J_{\rm ab})+{\rm g}(6J_{\rm b}+3J_{\rm ab})].
\end{aligned}
$$

References

[1] Edelstein A D, Kim C, Quadri S B, Kim K H, Browning V, Yu H Y, Maruyuma B and Everett K 1990 *Solid State Commun.* **76** 1379

[2] Krishnan R, Gupta H O, Lassri H, Sella C and Kaaboutchi J 1991 *J. Appl. Phys.* **70** 6421

[3] Bayreuther G, Bensch F and Kottler V 1996 *J. Appl. Phys.* **79** 4509

[4] Chou K W, Puzic A, Stoll H, Schütz G, Waeyenberge B V, Tyliszczak T, Rott K, Reiss G, Brückl H, Neudecker I, Weiss D and Back C H 2006 *J. Appl. Phys.* **99** 08F305

[5] Ekiz C 2008 *Physica* A **387** 1185

[6] Hickey L L and Mills D L 1986 *Phys. Rev.* B **33** 3329.

[7] Albuquerque E I, Sarmento E F and Tilley D F 1986 *Solid State Commun.* **58** 41

[8] Ferrnberg A M and Landau D P 1991 *J. Appl. Phys.* **70** 6125

[9] Jaščur M and Kaneyoshi T 1995 *Physica* A **220** 542

[10] Htoutou K, Ainane A and Saber M 2004 *J. Magn. Magn. Mater.* **269** 245

[11] Canko O, Kantar E and Keskin M 2009 *Physica* A **388** 28

[12] Strečka J, Dely J and Canova L 2009 *Physica* A **388** 2394

[13] Nakamura Y 2000 *Phys. Rev.* B **62** 11742.

[14] Albayrak E and Yilmaz S 2007 *J. Phys.: Condens. Matter* **19** 376212

[15] Bobák A and Dely J 2007 *J. Magn. Magn. Mater.* **310** 1419

[16] Albayrak E 2007 *Physica* B **391** 47

[17] Miao H, Wei G Z and Geng J 2009 *J. Magn. Magn. Mater.* **321** 413

[18] Miao H, Wei G Z, Liu J and Geng J 2009 *J. Magn. Magn. Mater.* **321** 102

[19] Kaneyoshi T 1993 *Acta Phys. Pol.* A **83** 703

[20] Hashimoto K and Ohkoshi S 1999 *Philos. Trans. R. Soc. London* A **357** 2977

[21] Callen H B 1963 *Phys. Lett.* **4** 161

[22] Kaneyoshi T 1986 *Phys. Rev.* B **33** 7688

[23] Honmura R and Kaneyoshi T 1979 *J. Phys.* C: *Solid State Phys.* **12** 3979

[24] Zernike F 1940 *Physica* **7** 565
[25] Kaneyoshi T, Jaščur M and Tomczak P 1993 *J. Phys.: Condens. Matter* **5** 5331
[26] Bobák A 1998 *Physica* A **258** 140
[27] Ez-Zahraouy H, Bahmad L and Benyoussef A 2006 *Braz. J. Phys.* **36** 557
[28] Albayrak E, Bulut T and Yilmaz S 2007 *J. Stat. Phys.* **127** 967
[29] Néel L 1948 *Ann. Phys.* **3** 137
[30] Chikazumi S 1997 *Physics of Ferromagnetism* (Oxford: Oxford University Press)
[31] Albayrak E and Bulut T 2007 *Physica* B **400** 124
[32] Deviren B, Canko O and Keskin M 2008 *J. Magn. Magn. Mater.* **320** 2291
[33] Deviren B, Akbudak S and Keskin M 2011 *Solid State Commun.* **151** 193
[34] Canko O and Albayrak E 2007 *Phys. Rev.* E **75** 011116
[35] Jensen P J, Bennemann K H, Poulpoulos P, Farle M, Wilhelm F and Baberschke K 1999 *Phys. Rev.* B **60** 14994
[36] Plascak J A, Moreira J G and Sá Barreto F C 1993 *Phys. Lett.* A **173** 360
[37] Godoy M, Leite V S and Figueiredo W 2004 *Phys. Rev.* E **69** 054428
[38] Keskin M and Ertaş M 2009 *Phys. Rev.* E **80** 061140
[39] Deviren B and Keskin M 2010 *J. Stat. Phys.* **140** 937
[40] Jiang L, Zhang J, Chen Z, Feng Q and Huang Z 2010 *Physica* B **405** 420